



Evaluation of DGT and DGT-PROFS modeling approach to estimate desorption kinetics of Cs in soils

Philippe Ciffroy, Loic Carasco, Daniel Orjollet, Caroline Simonucci, Laureline Fevrier

► To cite this version:

Philippe Ciffroy, Loic Carasco, Daniel Orjollet, Caroline Simonucci, Laureline Fevrier. Evaluation of DGT and DGT-PROFS modeling approach to estimate desorption kinetics of Cs in soils. Journal of Environmental Radioactivity, 2021, 235-236, pp.106646. 10.1016/j.jenvrad.2021.106646 . hal-03368651

HAL Id: hal-03368651

<https://hal.science/hal-03368651>

Submitted on 6 Oct 2021

HAL is a multi-disciplinary open access archive for the deposit and dissemination of scientific research documents, whether they are published or not. The documents may come from teaching and research institutions in France or abroad, or from public or private research centers.

L'archive ouverte pluridisciplinaire **HAL**, est destinée au dépôt et à la diffusion de documents scientifiques de niveau recherche, publiés ou non, émanant des établissements d'enseignement et de recherche français ou étrangers, des laboratoires publics ou privés.



Distributed under a Creative Commons Attribution - NonCommercial - NoDerivatives 4.0 International License

Evaluation of DGT and DGT-PROFS modeling approach to estimate desorption kinetics of Cs in soils

Ciffroy P.^{(1),*}, Carasco L.⁽²⁾, Orjollet D.⁽²⁾, Simonucci C.^{(3),(4)} and Février L.^{(2),*}

⁽¹⁾ EDF, Division Recherche et Développement, Laboratoire National d'Hydraulique et Environnement, 6 quai Watier, 78401 Chatou, France

⁽²⁾ Institut de Radioprotection et de Sûreté Nucléaire (IRSN), PRP-ENV, SRTE, LR2T, Cadarache, France

⁽³⁾ Institut de Radioprotection et de Sûreté Nucléaire (IRSN), PRP-ENV, SEDRE, LELI, Fontenay-aux-Roses, France

⁽⁴⁾ Present address: Institut de Radioprotection et de Sûreté Nucléaire (IRSN), PRP-ENV, SIRSE, LERNORD, Fontenay-aux-Roses, France

*Corresponding author: philippe.ciffroy@edf.fr; laureline.fevrier@irsn.fr

Accepted in Journal of Environmental Radioactivity

<https://doi.org/10.1016/j.jenvrad.2021.106646>

Abstract

The aim of this paper is to assess the suitability of DGT to extract kinetic rates of desorption of cesium (Cs) from soils. For this purpose, laboratory experiments with a natural soil spiked with Cs were carried out under three different contamination conditions, reflecting either an increase in Cs contamination level or an ageing of the contamination within the soil. The experimental results, i.e. the Cs accumulation kinetics onto DGT probes were interpreted by the DGT-PROFS model. The latter calculates the partitioning of Cs between two particulate pools, describing weak and strong interactions respectively, as well as kinetic rates describing exchange reactions. Experimental conditions did not show any major impact on desorption rates, suggesting that desorption kinetics were not significantly affected by contamination level and ageing. Instead, the distribution of Cs among

weak and strong sites was shown to be the predominant factor governing the differences observed in the remobilization of Cs to porewater among experimental conditions. The DGT technique combined with the DGT-PROFS modelling approach was proved to be efficient in estimating desorption kinetic rates of Cs in soils.

1. Introduction

¹³⁷Cs is an important fission product of the irradiation of uranium-based fuels. It is one of the most released radionuclides in the environment due to nuclear weapons testing or nuclear accidents, going from leakage from high level waste storage sites such as Hanford, USA (Zachara et al., 2002) or Mayak, Russia (Balonov et al., 2007) to large environmental spreading after Chernobyl or Fukushima accidents (Steinhauser et al., 2015; Beresford et al., 2016). Once released into the environment, ¹³⁷Cs penetrates the soil. Due to its chemical similarity with K, it can then be taken up by plants and enter the human food chain. Because of its high radioactivity and relative long half-life ($t_{1/2} = 30$ years), it represents a hazard for human health due both to internal contamination through food-chain and external exposure to gamma-ray. Therefore understanding its behaviour and predicting its mobility in the terrestrial environment is still of major importance.

In soils (or sediments), Cs interacts mainly with clay minerals, which contain highly selective sorption sites for alkali metals such as Cs and K (Evans et al., 1983; Cremers et al., 1988). Sorption of Cs on clay minerals involve multiple sites (including planar surface sites, edge sites, hydrated interlayer sites, frayed edge sites – FES - and interlayer sites) exhibiting different affinities and specificities for Cs (Okumura et al., 2018). The highest binding sites in terms of affinity, which are also the lowest in terms of density, are the so-called FES located at the wedge-shaped edges of micaceous clay minerals, particularly on illite. The involvement of sorption sites exhibiting different Cs capacities and affinities result in a non-linear sorption of Cs in soils as function of Cs concentration. Classical S-shape sorption isotherms are usually found; which means that the solid-liquid distribution of Cs depends on the concentration of Cs (Missana et al., 2014). Macroscopically, sorption of Cs on clay minerals (Brouwer et al., 1983; Poinssot et al., 1999; Bradbury and Bayens, 2000; Cherif et al., 2017; Siroux et al., 2018) but also onto complex phases (Cherif et al., 2017; Siroux et al., 2018; Wissocq et al., 2018), in soils (Missana et al., 2014) or in sediments (Fuller et al., 2014) has been successfully described by thermodynamic models assuming either surface complexation and/or ion exchange on reactive sites, two or three reactive sites, and an additivity of the reactive components.

If sorption of Cs on montmorillonite and kaolinite is expected to be reversible, sorption/desorption experiments highlighted an apparent irreversibility of Cs sorption on illite (Comans et al., 1991; Comans and Hockley, 1992). This behaviour has been interpreted as the result of the collapse of hydrated interlayers of illite in which the Cs was trapped or of the slow migration of Cs into core region of illite particles (Comans and Hockley, 1992; De Koning and Comans, 2004; Okumura et al., 2018). Recently Durrant et al. (2018) showed that desorption of Cs from illite is in fact totally reversible, at least for concentration of Cs in solution below 10^{-5} M. However the amount desorbed is very low due to the high values of affinity constants between Cs and illite. Besides, the outcome of the slow migration of Cs into core region of illite particles is that increased contact time between Cs and particles - or in other term the ageing of contamination - may decrease the amount of readily extractable Cs from illite (Fuller et al., 2015; Durrant et al., 2018; Okumura et al., 2018).

In addition to clay minerals, organic matter is another potential sorbent of Cs in soils. However, its role is still debatable and seems to depend on its content in soils. In soils with high organic matter content (>80%), it has been shown to play a significant role in Cs sorption (Valcke and Cremers, 1994; Rigol et al., 2002; Lofts et al., 2002). However, on soil containing less than 40 % of organic matter, Valcke and Cremers (1994) showed that the clays FES are the main sorption sites for Cs. Moreover, no data regarding the reversibility of Cs sorption on soil organic matter has been reported.

As a result, modelling the desorption dynamics of Cs in soils and sediments requires the description of at least two particulate pools with different interaction strengths and kinetics (Absalom et al., 1996; Ciffroy et al., 2003; Garnier et al., 2006; Murota et al., 2016). Only a very small pool of Cs is considered as readily desorbable (Kasar et al., 2020). The other pools are either considered as irreversibly fixed or following a very slow kinetic rate of desorption. As for clay minerals, ageing increased the stability of Cs sorption in soils and sediments and reduces the amount readily desorbable (Valcke and Cremers, 1994; Rigol et al., 1999a; Ciffroy et al., 2001; Al Attar et al., 2016; Tachi et al., 2020). Since Cs persists in the environment, quantifying the amount and rate of Cs release from soils is still of major importance to predict correctly the gradual migration of Cs in deeper soil horizons or the amount available for uptake by plants at long time scale (Murota et al., 2016; Brimo et al., 2019; Chaif et al., 2021).

Information on trace metals (TMs) exchange between soil particles and soil solution has already been assessed by using the diffusive gradient in thin-films (DGT) technique, which is a dynamic *in situ* sampling technique of labile TMs in solution (Zhang et al., 1998). The principle behind DGT is that the sampler provides a localized region of low metal concentration, which promotes a diffusive flux of TM into the sampler. Interpretation of TM fluxes into the DGT sampler indicates the degree of depletion of the metal concentration at the device interface, the kinetics of desorption of the metal, and the size

of the pool(s) of labile metal in the particulate phase. Interpretation of DGT measurements in soils requires a conceptual model of TMs sorption/desorption reactions and diffusion in soils (Cornu et al., 2007) as well as a numerical model for fitting geochemical parameters of concern. For this purpose, Harper et al. (1998) and Sochaczewski et al. (2007) developed the 'DGT-Induced Fluxes in Soils and Sediments' models (1D-DIFS and 2D-DIFS), which allow calculating the distribution ratio K_{dl} between fractions of TM respectively adsorbed on particles and dissolved in solution, and the response time T_c , which describes metal resupply kinetics from the solid phase. Despite their undisputable performance and wide dissemination among DGT users, the DIFS models showed flaws in some cases. Firstly, the DIFS model considers a single pool of labile adsorbed TM. Yet, it was shown that a single pair of forward and reverse rate constants is sometimes inaccurate and that multiple types of sorption sites should instead be used for describing multiple-stage kinetics (Ernstberger et al., 2002; Lehto et al., 2008; Nowack et al., 2004; Cornu et al., 2007; Mihalik et al., 2012). Secondly, it was shown in some cases that a number of combinations of K_{dl} and T_c can be fitted to an experimental data set with equivalent results (Lehto et al., 2008). To overcome such limitations, Ciffroy et al. (2011) developed the DGT-PROFS model. This model considers the soil (or sediment) as having two labile solid phases instead of one and advanced methods for probabilistic and sensitivity analysis, allowing us to represent parameters by Probability Distribution Functions (PDFs) instead of best estimates. These models are able to quantify TM partitioning between the pools they consider (Nia et al., 2011). In the case of DGT-PROFS model, the partitioning between two particulate pools, describing weak and strong interactions with TM, is thus calculated.

DGT was originally developed for divalent cations and its adaptation for other elements requires the development of specific resins. This explains limited applications of DGT for sampling Cs in natural environments (Chang et al., 1998; Murdock et al., 2001; Li et al., 2009; Gorny et al., 2019). In the time-restricted framework of the NEEDS-Environment funded projects, we therefore proposed to assess the ability of the DGT technique to be used to extract information on Cs desorption dynamics in soils. A set of kinetics laboratory experiments with a natural soil spiked with Cs was performed. The DGT-PROFS model was used to interpret the measurement and give insight into Cs desorption kinetic parameters. Regarding Cs sorption features described above, a special attention was given to the effects of Cs concentration and Cs contamination ageing on the desorption behaviour of Cs in soils.

2. Material and methods

2.1 Preparation of Cs-specific DGT

The DGT technique is described in detail in other papers (e.g. Davison and Zhang, 1994). Then, only the design of specific DGT samplers for Cs is described here.

AMP (Ammonium Molybdo Phosphate, $2\text{PO}_4(\text{NH}_4)_3\cdot 24\text{MoO}_3\cdot 3\text{H}_2\text{O}$) was selected as a reliable chelating gel material for sampling radiocesium (Murdock et al., 2001; Gorny et al., 2019). The chelating gels were acrylamide hydrogels, made using AMP, acrylamide monomer, ammonium persulfate initiator and TEMED catalyst according to the procedure described in Gorny et al. (2019). Diffusive gels were standard diffusive gel discs in agarose crosslinked polyacrylamide (APA) purchased from DGT Research Ltd. (Lancaster, UK); with a thickness of 0.78 mm. The gel was assembled in a standard plastic DGT holder with a window area of 2.54 cm^2 . A membrane filter with a $0.40\text{ }\mu\text{m}$ porosity (IsoporeTM Membrane Polycarbonate Filters) extended the DGT diffusive layer thickness by 0.13 mm and protected the gel from particles.

2.2 Soil spiking and deployment of DGT in soils

Soil used for the experiments was sampled at Auzerville (Haute Garonne, France) over a depth of 10 cm and was previously characterized by Devau et al. (2011). It was dried and sieved at 2 mm. The organic carbon concentration was measured by heat-loss weight at $1000\text{ }^\circ\text{C}$ whereas the cation exchange capacity (CEC) and the concentrations of the exchangeable cations were determined by extraction with cobalthexamine chloride. Its main physico-chemical characteristics are reported in Table 1. From a textural point of view, it is a silty-clay soil (with a clay content $> 35\%$). Among clay minerals, illite and kaolinite are the predominant ones (content around 10%), whereas montmorillonite content is about 4% of soil fraction below 2mm. This soil has a rather low organic carbon content, with a rate not exceeding 1%. Measurement of natural stable Cs background in this soil was not performed, since Cs from background was not expected to be mobile and to interfere in the experiments.

Table 1 - Physico-chemical characteristics of the soil used for the experiments

pH	6.53
Organic carbon (g.kg ⁻¹ dry weight)	9.82
CEC (cmol. kg ⁻¹ dry weight)	11.52
Ca (cmol. kg ⁻¹ dry weight)	9.31
Mg (cmol. kg ⁻¹ dry weight)	1.22
Na (cmol. kg ⁻¹ dry weight)	0.05
K (cmol. kg ⁻¹ dry weight)	0.71
Illite (g.kg ⁻¹ dry weight)	100
Montmorillonite (g.kg ⁻¹ dry weight)	39
Kaolinite (g.kg ⁻¹ dry weight)	101
Goethite (g.kg ⁻¹ dry weight)	4.9

Three spiking conditions were defined for generating contrasted contaminated soils. For each of these three conditions, 290 g dry weight of soil were spiked with a solution containing known and predefined quantities of stable cesium (¹³³Cs) and radiocesium (¹³⁷Cs). ¹³⁷Cs, which is naturally not present in this soil, was used to trace the behavior of freshly added Cs. The three conditions, hereafter noted conditions A, B, and C respectively, correspond to soils contaminated with the following levels:

- Condition A: 1.18.10⁻⁷ mol.g⁻¹ dry weight of total Cs (¹³³Cs and ¹³⁷Cs) and 1.93.10³ Bq.g⁻¹ dry weight of ¹³⁷Cs. The contaminated soil was used within three days after spiking;
- Condition B: 1.09.10⁻⁵ mol.g⁻¹ dry weight of total Cs (¹³³Cs and ¹³⁷Cs) and 1.94.10³ Bq.g⁻¹ dry weight of ¹³⁷Cs. The contaminated soil was used within three days after spiking;
- Condition C: 1.09.10⁻⁵ mol.g⁻¹ dry weight of total Cs (¹³³Cs and ¹³⁷Cs) and 1.94.10³ Bq.g⁻¹ dry weight of ¹³⁷Cs. The contaminated soil was stored during 3 months prior DGT kinetic experiments for studying the ageing effect.

After spiking procedure and equilibration period, contaminated soils were distributed in equal quantities (15 g dry weight) to plastic beakers with a diameter of 4.3 cm, representing soil depth ranging from 1 to 1.5 cm. Quantities of soils have been chosen to obtain a soil layer thickness higher than the DGT probe influence depth. The soil samples were then moistened until a fine water layer formed at the soil surface and incubated for one hour before DGT probes were deployed. Final gravimetric water content (mass water/mass dry soil) was about 48%.

2.3 Kinetic experiments and ^{137}Cs analyses

After the equilibration period, DGT devices were gently pressed into the soil until the filter of the device was in contact with the surface of the soil housing. The experimental units were then closed and incubated at constant temperature (20°C) in the dark in a thermostated chamber (Figure 1). The water content was kept constant during the whole incubation. The DGT devices were then removed from the soils at different contact times, i.e 4, 8, 16, 24 and 96 hours. Three replicates were analyzed for each condition and at each time point (noted X1, X2 and X3 hereafter). At time 4 and 96 hours, the porewater was extracted from 2.5 g of soil by centrifugation at 20 000 g for one hour. The volume of extracted porewater ranged between 200 and 450 μl . ^{137}Cs was analyzed by gamma-spectroscopy after acidification (using a pure germanium gamma spectrometer – Camberra). Quantity detected were always above the detection limit of the method.

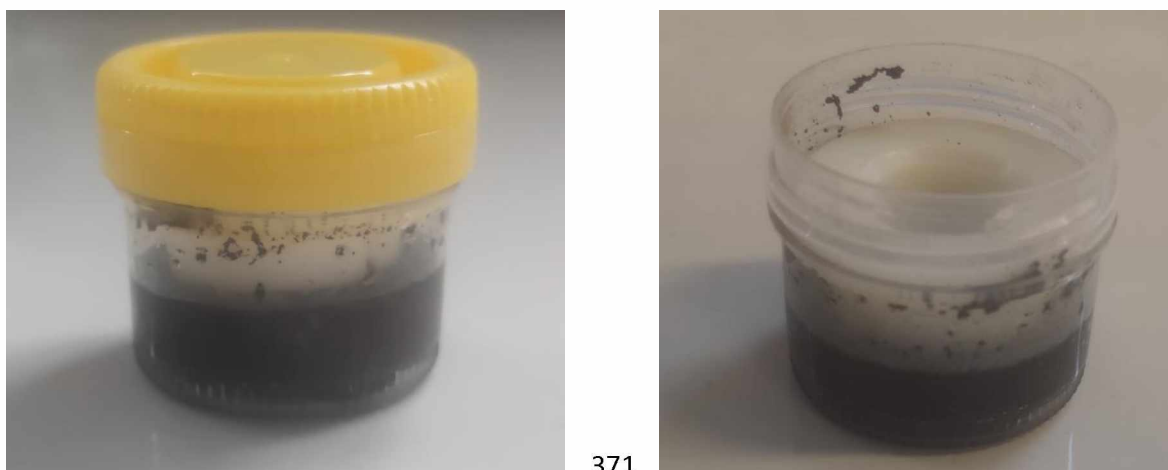


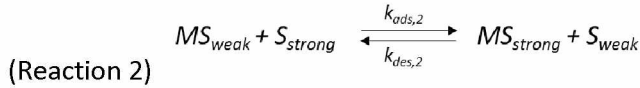
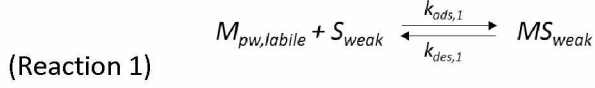
Figure 1 – Experimental device

After deployment, the DGT probes were retrieved and jet-washed with deionized water to remove soil particles before being disassembled. ^{137}Cs was analyzed directly on the chelating gel by gamma spectroscopy as described in Murdock et al. (2001).

2.4 DGT-PROFS modeling approach

The accumulation kinetics of Cs to DGT were interpreted by the DGT-PROFS model thoroughly described in Ciffroy et al. (2011). The model is coded with the Ecolego® tool (<https://www.ecolego.se/>). Briefly, the model considers that transport in both the diffusion layer (DGT gel) and soil porewater is solely driven by molecular diffusion and that all labile Cs species in porewater have a single self-diffusion coefficient. It is a one dimensional model operating along the axis perpendicular to the DGT interface. These assumptions are strictly the same as those considered by Harper et al. (1998) and

Harper et al. (2000) for the 1D-DIFS model. Unlike the DIFS model described in Harper et al. (1998), the DGT-PROFS model assumes that Cs in soil can be distributed between three separate phases: (i) porewater (where speciation may influence the diffusion coefficient values in soil solution and in DGT gel), (ii) weak and (iii) strong sorption sites on the particulate phase. This model assumes that interactions with weak and strong sites can be described by consecutive reactions (reactions 1 and 2):



where $M_{pw,labile}$ is labile Cs in the porewater (mol.cm^{-3}); S_{weak} and S_{strong} are particles weak and strong sites respectively (mol.g^{-1}); MS_{weak} and MS_{strong} are the concentration of Cs on the weak and strong particulate sites respectively (mol.g^{-1}); and $k_{ads,1}$, $k_{des,1}$, $k_{ads,2}$, $k_{des,2}$ are sorption-desorption rate constants on or from the weak and strong sites ($\text{g.mol}^{-1}.\text{s}^{-1}$; s^{-1} ; $\text{g.mol}^{-1}.\text{s}^{-1}$; $\text{g.mol}^{-1}.\text{s}^{-1}$, respectively).

To simplify the equations, the conditional rate constants $k_{ads,1}^*$, $k_{ads,2}^*$ and $k_{des,2}^*$ (s^{-1}) are defined depending on concentrations of the weak and strong available sites (S_{weak}) and (S_{strong}) as follows:

$$(Equation\ 1) \quad k_{ads,1}^* = k_{ads,1} \cdot (S_{weak})$$

$$(Equation\ 2) \quad k_{ads,2}^* = k_{ads,2} \cdot (S_{strong})$$

$$(Equation\ 3) \quad k_{des,1}^* = k_{des,1}$$

$$(Equation\ 4) \quad k_{des,2}^* = k_{des,2} \cdot (S_{weak})$$

The distribution of Cs between weak and strong sorption sites is described by α_{weak} , which indicates the proportion of Cs adsorbed onto the weak sites before DGT deployment:

$$(Equation\ 5) \quad \alpha_{weak} = \frac{(MS_{weak})_{t=0}}{(MS_{weak})_{t=0} + (MS_{strong})_{t=0}}$$

The accumulation of Cs on DGT is governed by the adsorption-desorption kinetics described in reactions 1 and 2, and by the diffusion of Cs within soil porewater and DGT gel. Diffusion in soil and chemical reactions lead to the following set of mass-balance equations:

$$(Equation\ 6) \quad \frac{\partial(M_{pw,labile})}{\partial t} = D_{sed} \cdot \frac{\partial^2(M_{pw,labile})}{\partial x^2} - k_{ads,1}^* (M_{pw,labile}) + k_{des,1}^* \cdot Sed. (MS_{weak})$$

$$(Equation\ 7) \quad \frac{\partial(MS_{weak})}{\partial t} = \frac{k_{ads,1}^* (M_{pw,labile})}{Sed} - (k_{des,1}^* + k_{ads,2}^*) (MS_{weak}) + k_{des,2}^* (MS_{strong})$$

$$(Equation\ 8) \quad \frac{\partial(MS_{strong})}{\partial t} = k_{ads,2}^* (MS_{weak}) - k_{des,2}^* (MS_{strong})$$

410 where D_{sed} is the apparent diffusion coefficient of Cs in soil ($\text{cm}^2.\text{s}^{-1}$) and Sed is the concentration of
411 particles in soil ($\text{g}.\text{cm}^{-3}$).

412 Only labile Cs, $M_{pw,labile}$, (i.e., free Cs and small inorganic complexes able to dissociate in the gel) are
413 assumed to diffuse in the DGT gel, with only one kinetic equation describing transport in the diffusive
414 layer of the DGT device:

415 (Equation 9)
$$\frac{\partial(M_{pw,labile})}{\partial t} = D_{gel} \cdot \frac{\partial^2(M_{pw,labile})}{\partial x^2}$$

416 where D_{gel} is the apparent diffusion coefficient of Cs in the DGT gel ($\text{cm}^2.\text{s}^{-1}$).

417 In the specific case of Cs however, speciation in soil porewater (e.g. eventual complexation with
418 organic matter) was not considered because Cs shows poor affinity with dissolved organic matter and
419 remains mainly under its free species Cs^+ form. Therefore, D_{gel} was taken equal to the diffusion
420 coefficient of Cs^+ in water D_{water} . D_{sed} was derived from the coefficient of Cs^+ in water corrected to
421 account for the tortuosity during the diffusion in the soil layer, according to the Millington and Quirk's
422 relationship, which states that tortuosity depends on porosity φ and water content θ :

423 (Equation 10)
$$D_{sed} = \text{Tortuosity} \cdot D_{water} = \frac{\theta^{10/3}}{\varphi^2} \cdot D_{water}$$

424 Equations at the interface soil-DGT are built according to the same principles presented in Harper et
425 al. (1998).

426

427 2.5 Calibration of the DGT-PROFS model parameters

428 In summary, the model is described by five parameters, i.e. the kinetic parameters $k_{ads,1}^*$, $k_{des,1}^*$, $k_{ads,2}^*$
429 and $k_{des,2}^*$, and the proportion of particulate Cs associated to weak sites α_{weak} . Only a few
430 experimental data are available for each experiment (i.e. Cs accumulated on DGT at different times).
431 So additional reasonable assumptions were considered to reduce the number of parameters to be
432 fitted. The first assumption is that the sediment is under equilibrium conditions before the deployment
433 of the DGT device, i.e. $\left[\frac{\partial(M_{Sstrong})}{\partial t} \right]_{t=0} = 0$. Equation (8) can then be written:

434 (Equation 11)
$$\frac{(M_{Sstrong})_{t=0}}{(M_{Sweak})_{t=0}} = \frac{k_{ads,2}^*}{k_{des,2}^*} = \frac{1-\alpha_{weak}}{\alpha_{weak}}$$

435 The value of $k_{ads,2}^*$ can then be derived from $k_{des,2}^*$ and α_{weak} .

436 Similarly, it can be assumed that the sediment-water system is at equilibrium and that no diffusion
437 occurs before DGT deployment, i.e. $\frac{\partial(M_{pw,labile})}{\partial t} = 0$. Equation (6) can then be written:

438 (Equation 12)
$$\frac{(MS_{weak})_{t=0}}{(M_{pw,labile})_{t=0}} = \frac{k_{ads,1}^*}{k_{des,1}^* \cdot Sed} = \alpha_{weak} \cdot \frac{(MS_{weak})_{t=0} + (MS_{strong})_{t=0}}{(M_{pw,labile})_{t=0}} = \alpha_{weak} \cdot K_{d,0}$$

439 where $K_{d,0}$ is the distribution coefficient of Cs between the solid and liquid phase at the beginning of
440 the experiment.

441 The value of $k_{ads,1}^*$ can then be derived from $k_{des,1}^*$, α_{weak} and from the observed ratio between
442 particulate and dissolved cesium at initial time.

443 Then, for each soil condition, the DGT-PROFS model allows one to fit the following parameters: α_{weak} ,
444 the proportion of particulate Cs associated to weak sites; $k_{des,1}^*$, the desorption rate from weak
445 particulate sites; and $k_{des,2}^*$, the desorption rate from strong particulate sites.

446 These parameters can be obtained by fitting the DGT experimental measurements using a probabilistic
447 approach described in detail in Ciffroy et al. (2011). We remind here the main principles of the
448 calibration approach. A great number of $\{\alpha_{weak}; k_{des,1}^*; k_{des,2}^*\}$ combinations (10000 combinations)
449 were randomly sampled within a large range of potential parameter values (e.g. α_{weak} is randomly
450 sampled from 0 to 1) and the model was run for each of them. For each combination, the error of
451 prediction was calculated as the sum of squared distances between measured and experimental Cs
452 concentrations on DGT. The $\{\alpha_{weak}; k_{des,1}^*; k_{des,2}^*\}$ combinations were then ranked from those given
453 the lowest error to those given the highest one. The top 100 best combinations were selected and
454 weighted for building PDFs for each of the three investigated parameters according to the procedure
455 described in Ciffroy et al (2011). In conclusion, this method allows us to represent parameters by PDFs
456 (i.e., with indications of their uncertainty) instead of single values.

457

458 3. Results

459 3.1 Cs initial distribution in soils

460 It is assumed that the Cs depletion induced in the soil porewater for short exposure time occurred on
461 a limited distance from the DGT interface (Harper et al., 2000). Therefore concentration of Cs in the
462 soil porewater extracted by centrifugation at time 4 was considered as not impacted by the presence
463 of DGT and used as a surrogate of the concentration of Cs in the soil porewater at the beginning of the
464 experiments. These concentrations were respectively $4.32 \times 10^{-7} \pm 9.3 \times 10^{-8}$ mol.L⁻¹, $3.28 \times 10^{-4} \pm 1 \times$
465 10^{-5} mol.L⁻¹ and $3.28 \times 10^{-4} \pm 8.5 \times 10^{-6}$ mol.L⁻¹ in conditions A, B and C respectively. It corresponds to
466 0.16 ± 0.03 % of total Cs in the soil in condition A, while it represents 1.42 ± 0.01 and 1.64 ± 0.04 % for
467 conditions B and C respectively showing that most part of Cs was sorbed to the soil particles.
468 Concentration of Cs in soil porewater can be used to calculate the distribution coefficient K_d , defined

as the ratio between Cs concentration sorbed on particles to the Cs concentration in the soil porewater. The values ranged between 282 ± 69 , 33 ± 1 and 33 ± 1 L.kg⁻¹ for condition A, B and C respectively. K_d for condition A is in accordance with the mean K_d value reported by IAEA (IAEA, 2010) for Cs in silty-clay soils, whereas K_d for condition B and C are slightly lower than the minimal value reported by IAEA (that is 39 L.kg⁻¹).

Total concentration of Cs impacted highly the liquid-solid distribution of Cs within this soil, with one order of difference in K_d between condition A and B. Such behaviour relates to the non-linear sorption of Cs as a function of concentration (Missana et al., 2014). Concentrations of Cs used in this study have been chosen based on previous works on the same soil (Cherif, 2017) in order to cover different parts of Cs sorption isotherm. As expected, our K_d values are in agreement with those reported by Cherif (2017). This author conducted 48h contact-time sorption experiments and showed a decrease of K_d from more than 3000 L.kg⁻¹ for small concentration of Cs to about 30 L.kg⁻¹ for high concentration of Cs. Condition A reproduced conditions of low Cs concentrations just above the inflection point of the sorption isotherm (around 10⁻⁷ mol.L⁻¹) whereas condition B reproduced conditions of high Cs concentrations.

Effect of contamination ageing was not evidenced from the solid-liquid distribution of Cs, as seen from the comparison of K_d in condition B and C. Some authors showed that ageing effect was more pronounced in organic than in mineral soils (Rigol et al., 1999b). However while K_d values allow us to measure the capacity of soils to sorb Cs, desorption experiments are necessary to assess the reversibility of Cs adsorption (a low or a high K_d value being not in itself an indicator of the reversibility of sorption or of the absence of kinetically-controlled interactions with soil particles) and highlight potential ageing effect (Gil-Garcia et al., 2008).

Based on previous results of Cherif (2017), where evolution of soil solution chemistry has been measured during sorption/desorption experiments, no modification due to biogeochemical processes (for ex. soil solution chemistry changes induced by soil microbiology) was expected to have impacted our results during the DGT exposure time.

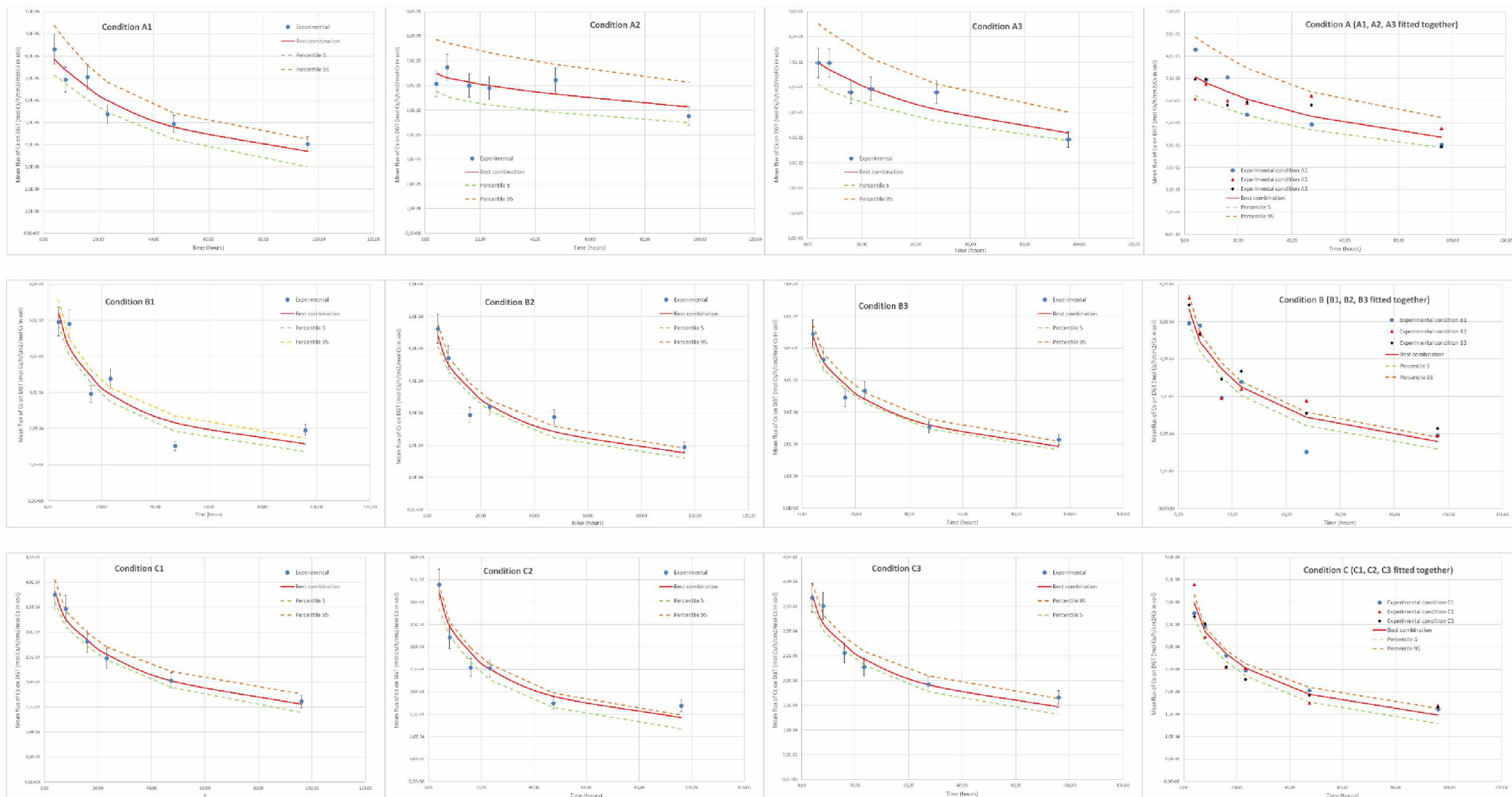
3.2 Cs flux to DGT

The measured flux of Cs to the DGT resin over time for the three experimental conditions and their replicates is shown in Figure 2. To facilitate the comparison between the experiments and the replicates, results are normalized to the total amount of Cs in soil (i.e. 'Mean flux of Cs onto DGT' is expressed in mol Cs onto DGT.h⁻¹.cm⁻².mol⁻¹ of total Cs in soil before DGT implementation). Cs flux on DGT followed similar shapes for all conditions, except for experiment A2 showing a relatively stable

flux over time. They are characterized by a continuous decline of Cs flux onto DGT resin over time, this trend being more significant for conditions B and C. According to the qualitative classification defined by Harper et al. (2000), these conditions can be considered representative of ‘diffusive’ or ‘partial-non-steady state’ cases: the DGT device progressively depletes porewater concentrations while the resupply from particles cannot be sustained (in opposition to ‘sustained’ or ‘partial’ systems, where the resupply is sufficiently fast so as to maintain a constant flux to DGT over time). This double effect (depletion in porewater not totally sustained by desorption from particles) explains the progressive decrease of accumulation rate on DGT. Nevertheless, even if the shapes were similar, different levels and slopes were observed for conditions A, B and C with flux decreasing from about 7×10^{-5} to 4×10^{-5} mol.h⁻¹.cm⁻².mol⁻¹ Cs in soil for condition A, from about 6×10^{-4} to 2×10^{-4} for condition B and from about 4×10^{-4} to 1.5×10^{-4} for condition C. In accordance with these fluxes, Cs trapped by DGT after 96h of deployment represented $1.03 \pm 0.11\%$ of total Cs in soil in condition A, $4.79 \pm 0.28\%$ in condition B and $4.05 \pm 0.15\%$ in condition C. Few studies have been devoted up to date to study desorption kinetics of Cs in soils. Liu et al. (2003) observed also a two-step kinetics of Cs desorption from contaminated sediments sampled at Hanford Site. The first stage consisting of a rapid initial release of Cs was followed by a slow kinetic one. Recently Murota et al. (2016) recorded the same pattern of desorption kinetics on natural Japanese soils contaminated by the Fukushima nuclear accident using the “infinite bath” technique of Wauters et al. (1994). In this technique, Cs released in soil solution is immediately captured by a sorbent, which like DGT stimulates desorption by maintaining a virtually “zero” concentration of Cs in soil solution. They found a continuous release of Cs from soils during 139 days, but with desorption fluxes decreasing with time.

Effect of contamination level on yield of desorption and Cs flux to DGT was evidenced by the comparison of condition A and B, with fluxes about one order of magnitude higher in condition with a high level of Cs contamination. An increase in desorption yield with an increase in Cs contamination level was frequently found in literature (Durrant et al., 2018; Tachi et al., 2020).

Effect of ageing was less clear, but a lower flux rate was recorded in condition C compared to condition B, leading to a smaller amount of Cs extracted by DGT upon 96 hours. While less release of Cs following increased contact time with Cs contamination has been reported by several authors on soils (Valcke and Cremers, 1994; Roig et al., 2007; Al Attar et al., 2016; Murota et al., 2016), or sediments (Ciffroy et al., 2001), others failed to demonstrate it (Zachara et al., 2002). As stated previously, impact of ageing may depend on soil nature and particularly on the content of organic matter (Rigol et al., 1999a; Roig et al., 2007).



537 **Figure 2** – Mean flux of Cs onto DGT (in $\text{mol Cs} \cdot \text{d}^{-1} \cdot \text{cm}^{-2} \cdot \text{mol}^{-1} \text{Cs in soil}$). The points represent experiment data – The continuous line represents the curve
 538 obtained with the best combination of parameter values - The upper and lower dotted lines represent the 5th and 95th percentiles, respectively

Decreases in fluxes with time, as well as difference in fluxes induced by Cs contamination level and ageing, probably result from different distribution of Cs on soil solid particles, with the involvement of multiple sites with different binding affinities for Cs. The objective of the modelling work described below is to quantify these differences, assuming the existence of two kind of binding sites (weak and strong sites), as well as the kinetic desorption rates associated to these sites.

3.3 Modeling results and interpretation of parameter values

The model previously described was calibrated for each of the experiments, i.e. for the three replicates of each condition, as well as for each condition A, B and C considering all replicates together. For any deployment time of the DGT, the comparison between model and experimental flux onto DGT is reported in Figure 2. The continuous line in Figure 2 represents the calculated flux kinetics obtained with the best combination of parameter values, while the upper and lower dotted lines represent the 5th and 95th percentiles, respectively. Results demonstrate that the average curve generally agrees well with experimental data and that the area encompassed by the 5th and the 95th percentiles includes experimental data points (except for experimental outliers like in experiment B1 and B2).

Fitted parameter values, i.e. the values of the desorption kinetic rates $k_{des,1}^*$ and $k_{des,2}^*$, as well as the proportion of Cs adsorbed onto the weak sites α_{weak} , are reported in Table 2. First, it can be noted that the standard deviations calculated for the normal PDFs reported in Table 2 are generally low. That means that the top 100 best $\{\alpha_{weak}; k_{des,1}^*; k_{des,2}^*\}$ combinations identified in the calibration procedure are quite homogeneous. The range of simulated parameter values is thus generally tight revealing that the uncertainty in the prediction is low. Variability on $k_{des,1}^*$ and $k_{des,2}^*$ between replicates for a given condition is also very limited, except in condition A where experiment A2 showed a specific pattern.

Experimental conditions did not show any major impact on desorption rates, $k_{des,1}^*$ and $k_{des,2}^*$, which remained generally on similar orders of magnitude: when considering mean values of the calculated PDFs (Table 2) (excepting experiment A2), $k_{des,1}^*$ ranges between 9.4×10^{-6} (condition A3) and 5×10^{-5} (condition B1) s⁻¹ and $k_{des,2}^*$ ranges from 4.8×10^{-8} to 5×10^{-8} s⁻¹ (Table 2). A slight effect of contamination level may appear on $k_{des,1}^*$ with lower values of desorption from the weak sites at low Cs concentration. However due to the high dispersion of data in condition A, this findings must be taken cautiously. Desorption rate constants from the stronger site are not affected by contamination level and ageing. Desorption rate constant is conceptually an intrinsic property of the site involved in sorption. Thus as long as these sites remain the same between our conditions, no change in $k_{des,1}^*$ or

$k_{des,2}^*$ was expected. However involvement of different sorption sites depending on the tested conditions would have resulted in different $k_{des,1}^*$ or $k_{des,2}^*$. Sorption of Cs at high concentration could have involved exchangeable sites non-solicited at lower Cs concentration. This assumption cannot be ruled out by comparing values of $k_{des,1}^*$ between condition A and B.

Table 2 - Calculated parameters with the DGT-PROFS model for the different conditions tested
 $\mathcal{N}(\mu; \sigma)$ is the normal distribution with the mean μ and the standard distribution σ

Condition	Ratio between Cs associated to weak sites to total particulate Cs: α_{weak} (-)	$k_{des,1}^*$ (s ⁻¹) Desorption rate from weak sites:	$k_{des,2}^*$ (s ⁻¹) Desorption rate from strong sites:
A1	$\mathcal{N}(0.14; 0.024)$	$\mathcal{N}(3.1.10^{-5}; 1.1.10^{-5})$	$\mathcal{N}(5.10^{-8}; 2.5.10^{-8})$
A2	$\mathcal{N}(0.49; 0.1)$	$\mathcal{N}(2.6.10^{-6}; 6.6.10^{-7})$	$\mathcal{N}(5.10^{-8}; 2.5.10^{-8})$
A3	$\mathcal{N}(0.22; 0.04)$	$\mathcal{N}(9.4.10^{-6}; 3.10^{-6})$	$\mathcal{N}(4.9.10^{-8}; 2.4.10^{-8})$
<i>A (A1, A2 and A3 fitted together)</i>	$\mathcal{N}(0.23; 0.05)$	$\mathcal{N}(9.9.10^{-6}; 3.2.10^{-6})$	$\mathcal{N}(4.9.10^{-8}; 2.5.10^{-8})$
B1	$\mathcal{N}(0.29; 0.023)$	$\mathcal{N}(5.10^{-5}; 1.10^{-5})$	$\mathcal{N}(5.10^{-8}; 2.5.10^{-8})$
B2	$\mathcal{N}(0.36; 0.03)$	$\mathcal{N}(4.1.10^{-5}; 7.9.10^{-6})$	$\mathcal{N}(4.9.10^{-8}; 2.5.10^{-8})$
B3	$\mathcal{N}(0.40; 0.03)$	$\mathcal{N}(3.2.10^{-5}; 5.7.10^{-6})$	$\mathcal{N}(4.9.10^{-8}; 2.4.10^{-8})$
<i>B (B1, B2 and B3 fitted together)</i>	$\mathcal{N}(0.35; 0.03)$	$\mathcal{N}(3.9.10^{-5}; 7.7.10^{-6})$	$\mathcal{N}(4.9.10^{-8}; 2.5.10^{-8})$
C1	$\mathcal{N}(0.24; 0.04)$	$\mathcal{N}(1.55.10^{-5}; 4.6.10^{-6})$	$\mathcal{N}(4.8.10^{-8}; 2.4.10^{-8})$
C2	$\mathcal{N}(0.17; 0.02)$	$\mathcal{N}(3.2.10^{-5}; 9.10^{-6})$	$\mathcal{N}(4.9.10^{-8}; 2.4.10^{-8})$
C3	$\mathcal{N}(0.19; 0.03)$	$\mathcal{N}(1.63.10^{-5}; 4.8.10^{-6})$	$\mathcal{N}(5.10^{-8}; 2.5.10^{-8})$
<i>C (C1, C2 and C3 fitted together)</i>	$\mathcal{N}(0.20; 0.03)$	$\mathcal{N}(2.10^{-5}; 6.10^{-6})$	$\mathcal{N}(5.10^{-8}; 2.5.10^{-8})$

Comparing desorption rates to already published data is difficult due to the small number of studies devoted to Cs desorption kinetics in natural soils. Most studies that have considered chemical kinetic reactions for sorption/desorption of Cs in soils or sediments have proposed models based on two sites, with one site at equilibrium with the porewater and one site involving either a kinetics of sorption and no desorption (meaning Cs is irreversibly fixed on this second site) or kinetics for both sorption and desorption, like in this study. Thus few authors have considered the existence of kinetic reactions on

two sites. Murota et al. (2016) have assumed the existence of three successive sites with Cs desorption following a pseudo first-order reaction kinetics from all of them. They used their models to describe results of Cs desorption from Japanese soils, contaminated with ^{137}Cs following the Fukushima-Daichi nuclear power plant accident, acquired through the “infinite bath” technique (Wauters et al., 1994), which make them particularly relevant to be compared to our results acquired with DGT. The average desorption rates for their three sites are 1×10^{-8} , 7×10^{-7} , and $4.5 \times 10^{-6} \text{ s}^{-1}$, from the stronger to the weaker sites respectively. Absalom et al. (1996) studied the dynamics of ^{137}Cs sorption/desorption in artificially contaminated organic and mineral soils, with a three box model. They reported a kinetic rate of desorption from “strong-like” sites of $1.7 \times 10^{-8} \text{ s}^{-1}$ in a mineral soil, while it was one order of magnitude higher for organic soils. In our study, $k_{des,2}^*$ values are in good agreement with desorption rate constants reported for strong sites by Murota et al. (2016) and Absalom et al. (1996) on soils. They fell also within the range of desorption rate constant reported from natural sediments ($1.2 \times 10^{-8} \text{ s}^{-1}$) by Liu et al. (2003). These slow desorption rates is assumed to be a consequence of the diffusion of Cs within interlayer of illite or other micaceous minerals (Murota et al., 2016, Okumura et al., 2018). As said previously, comparing $k_{des,1}^*$ to published data is difficult since in most multi-sites models, the first site is supposed to be an exchangeable site in equilibrium with soil porewater; exhibiting therefore no kinetic limitation. However our values of $k_{des,1}^*$ encompass the desorption rate constant proposed by Murota et al. (2016) for their weaker site as previously mentioned.

Effect of contamination level or ageing was expected on the distribution of Cs among weak and strong sites. Significant differences were indeed obtained on the fraction of Cs associated to weak sites, α_{weak} . Higher α_{weak} values were obtained for condition B (mean values: 29 to 40 %; 35% when all replicates are calibrated together, with a 90% confidence interval ranging from 29 to 41%), while only a small fraction of Cs is associated to weak sites under condition A1 and A3 (14 and 22% respectively; 23% when all replicates are calibrated together, with a 90% confidence interval ranging from 13 to 32%). All these results should be taken with caution since parameter values show variability among replicates, especially in condition A where the concentration of Cs was low. Such a variability may be explained by the fact that DGT accumulation is influenced by local conditions at the interface between the DGT membrane and soil and that a greater number of replicates would be necessary to improve the robustness of the evaluation. But it could also relate to the very small quantity of Cs recovered by DGT in condition A and the higher analytical uncertainty in this condition. Anyway the increase in α_{weak} with increasing Cs contamination can be explained by saturation of sorption sites on clay particles. Indeed, FES sites, which are the sites with the strongest Cs affinity, are also the smaller in terms of density. Therefore, when the contamination level is too high (conditions B and C), FES sites are saturated, leading to a redistribution of Cs among sorption sites present at the planar surface,

surface of frayed edge sites and/or strong interlayer (Missana et al., 2014; Cherif, 2017). With ageing, Cs is supposed to move into core region of illite particles. Therefore a decrease of α_{weak} was expected. While simple graphical analysis of results did not put in evidence ageing effect, modelling results indicate that the α_{weak} slightly decreased between conditions B and C from 35% (90% confidence interval [0.29-0.41]) to 20% (90% confidence interval [0.14-0.26]) when all replicates are calibrated together).

4. Conclusion

Predicting the dynamics of Cs at the particle/porewater interface in soils is an important task since this interaction partly controls its subsequent bioavailability to plants or soil organisms, but also migration to deeper soil horizons. A kinetic DGT experimental approach combined to the interpretation with the DGT-PROFS model was able to predict Cs dynamics at the particle-porewater interface of soils under various conditions. It was shown that the resupply of Cs to porewater from soil solid phases was modified according to contamination level, and that a slight ageing effect was put in evidence. The DGT-PROFS model showed that desorption kinetic rates were not significantly modified by contamination level and ageing. Cs partitioning between weak and strong adsorption sites was instead influenced by the contamination level, suggesting saturation effects. These results acquired on one soil should be further confirmed by studying soils with different properties. Content of clays and organic matter, but also nature of clay minerals, are known to be the main parameters controlling Cs sorption/desorption in soils. However this study demonstrates the suitability of DGT combined with a multi-compartmental model to extract parameters describing Cs desorption dynamic in soils. Such parameters can be further used in radioecological transfer model to predict Cs mobility or assess Cs impact in terrestrial ecosystem.

Acknowledgments

The authors would like to thank the French NEEDS-Environment program for funding the TECHMO-3D (Modélisation Dynamique de la Disponibilité du césium dans le sol : interprétation des flux de Cs à l'aide de mesures DGT) project.

References

- Absalom J.P., Crout N.M.J., Young S.D., 1996. Modeling radiocesium fixation in upland organic soils of Northwest England. *Environ. Sci. Technol.* 30, 2735–2741
- Al Attar L., Al-Oudat M., Safia B., Ghani B.A. 2016. Ageing impact on the transfer factor of ^{137}Cs and ^{90}Sr to lettuce and winter wheat. *J. Environ. Radioact.* 164: 19-25
- Balonov M.I., Bruk G.Y., Golikov V.Y., Barkovsky A.N., Kravtsova E.M., Kravtsova O.S., Mubasarov A.A., Shutov V.N., Travnikova I.G., Howard B.J., Brown J.E., Strand P. 2007. Assessment of current exposure of the population living in the Techa river basin from radioactive releases of the Mayak facility. *Health Physics* 92: 134-147
- Beresford N.A., Fesenko S., Konoplev A., Skuterud L., Smith J.T., Voigt G. 2016. Thirty years after the Chernobyl accident: What lessons have we learnt? *J. Environ. Radioact.* 157: 77-89
- Bradbury M.H. and Baeyens B. 2000. A generalised sorption model for the concentration dependent uptake of caesium by argillaceous rocks. *J. Cont. Hydrol.* 42: 141-163
- Brimo K., Gonze M-A., Pourcelot L. 2019. Long term decrease of ^{137}Cs bioavailability in French pastures: Results from 25 years of monitoring. *J. Environ. Radioact.* 208–209: 106029
- Brouwer E., Baeyens B., Maes A., Cremers A. 1983. Cesium and rubidium ion equilibrium on illite clays. *The Journal of Physical Chemistry* 87: 1213-1219
- Chaif H., Coppin F., Bahi A., Garcia-Sanchez L. 2021. Influence of non-equilibrium sorption on the vertical migration of ^{137}Cs in forest mineral soils of Fukushima prefecture. *J. Environ. Radioact.* 232: 106567
- Chang L-Y., Davison W., Zhang H., Kelly M. 1998. Document Performance characteristics for the measurement of Cs and Sr by diffusive gradients in thin films (DGT). *Anal. Chim. Acta* 368: 243-253
- Cherif M.A. 2017. Modélisation dynamique de la (bio)disponibilité des radionucléides dans les sols : approche comparative modèles-expériences appliquée au transfert de césium dans la rhizosphère. PhD thesis. Aix-Marseille University
- Cherif M.A., Martin-Garin A., Gérard F., Bildstein O. 2017. A robust and parsimonious model for caesium sorption on clay minerals and natural clay materials. *Appl. Geochem.* 87: 22-37
- Ciffroy P., Garnier J-M., Pham M. K. 2001. Kinetics of the adsorption and desorption of radionuclides of Co, Mn, Cs, Fe, Ag and Cd in freshwater systems: experimental and modelling approaches. *J. Environ. Radioact.* 55: 71-91

- Ciffroy P., Garnier J-M., Benyahya L. 2003. Kinetic partitioning of Co, Mn, Cs, Fe, Ag, Zn and Cd in fresh waters (Loire) mixed with brackish waters (Loire estuary): experimental and modelling approaches. *Mar. Pollut. Bulletin* 46: 626-641
- Ciffroy P., Nia Y., Garnier J-M. 2011. Probabilistic multicompartamental model for interpreting DGT kinetics in sediments. *Environ. Sci. Technol.* 45: 9558-9565
- Comans R., Hockley D. 1992. Kinetics of cesium sorption on illite. *Geochim. Cosmochim. Acta*, 56, 1157–1164
- Comans R.N., Haller M., De Preter P. 1991. Sorption of cesium on illite: non-equilibrium behaviour and reversibility. *Geochim. Cosmochim. Acta* 55(2), 433-440
- Cornu J-Y., Denaix L., Schneider A., Pellerin S. 2007. Temporal evolution of redox processes and free Cd dynamics in a metal contaminated soil after rewetting. *Chemosphere*, 70, 306–314
- Cremers A., Elsen A., De Preter P., Maes A. 1988. Quantitative analysis of radiocaesium retention in soils. *Nature* 335: 247–249
- Davison W., Zhang H. 1994. In situ speciation measurements of trace components in natural waters using thin-film gels. *Nature* 367: 546-548
- De Koning A., Comans R.N. 2004. Reversibility of radiocaesium sorption on illite. *Geochim. Cosmochim. Acta* 68 (13), 2815–2823.
- Devau N., Le Cadre E., Hinsinger P., Gérard F. 2011. Fertilization and pH effects on processes and mechanisms controlling dissolved inorganic phosphorus in soils. *Geochim. Cosmochim. Acta* 75: 2980-2996
- Durrant C.B., Begg J.D., Kersting A.B., Zavarin M. 2018. Cesium sorption reversibility and kinetics on illite, montmorillonite and kaolinite. *Sci. Total Environ.* 610-611: 511–520
- Ernstberger H., Davison W., Zhang H., Tye A., Young S. 2002. Measurement and Dynamic Modeling of Trace Metal Mobilization in Soils Using DGT and DIFS. *Environ. Sci. Technol.* 36: 349–354
- Evans C.H., Alberts J.J., Clark R.A. 1983. Reversible ion-exchange fixation of Cs-137 leading to mobilisation from reservoir sediments. *Geochim. Cosmochim. Acta* 47: 1041–1049
- Fuller A.J., Shaw S., Peacock C.L., Trivedi D., Small J.S., Abrahamsen L.G., Burke I.T. 2014. Ionic strength and pH dependent multi-site sorption of Cs onto a micaceous aquifer sediment *Applied Geochem.* 40: 32-42

- Fuller A.J., Shaw S., Ward M.B., Haigh S.J., Mosselmans F.W., Peacock C.L., Stackhouse S., Dent A.J., Trivedi D., Burke I.T. 2015. Caesium incorporation and retention in illite interlayers. *Appl. Clay Sci.* 108: 128–134
- Garnier J-M., Ciffroy P., Benyahya L. 2006. Implications of short and long term (30 days) sorption on the desorption kinetic of trace metals (Cd, Zn, Co, Mn, Fe, Ag, Cs) associated with river suspended matter. *Sci. Tot. Environ.* 366: 350-360
- Gil-Garcia C.J., Rigol A., Rauret G., Vidal M. 2008. Radionuclide sorption–desorption pattern in soils from Spain. *Appl. Rad. Isot.* 66: 126–138
- Gorny J., Gourgiotis A., Coppin F., Février L., Zhang H., Simonucci C. 2019. Better understanding and applications of ammonium 12-molybdophosphate-based diffusive gradient in thin film techniques for measuring Cs in waters. *Environ. Sci. Pollut. Res.* 26: 1994-2006
- Harper M.P., Davison W., Zhang H., Tych W. 1998. Kinetics of metal exchange between solids and solutions in sediments and soils interpreted from DGT measured fluxes. *Geochim. Cosmochim. Acta* 62: 2757–2770
- Harper M.P., Davison W., Tych W. 2000. DIFS - A modelling and simulation tool for DGT induced trace metal remobilisation in sediments and soils. *Environ. Model. Software* 15: 55-66
- IAEA (International Atomic Energy Agency). 2010. Handbook of Parameter Values for the Prediction of Radionuclide Transfer in Terrestrial and Freshwater Environments. 978-92-0-113009-9 Technical Reports Series No. 472
- Kasar S., Mishra S., Omori Y., Sahoo S.K., Kavasi N., Arae H., Sorimachi A., Aono T. 2020 Sorption and desorption studies of Cs and Sr in contaminated soil samples around Fukushima Daiichi Nuclear Power Plant. *J. Soils Sediments* 20: 392–403
- Lehto N.J., Davison W., Tych W., Zhang H. 2008. Quantitative assessment of soil parameter (KD and TC) estimation using DGT measurements and the 2D DIFS model. *Chemosphere*, 71, 795–801
- Li W., Wang F., Zhang W., Evans D. 2009. Measurement of stable and radioactive cesium in natural waters by the diffusive gradients in thin films technique with new selective binding phases. *Anal. Chem.* 81: 5889-5895
- Liu C., Zachara J.M., Smith S.C., Mc Kinley J.P., Ainsworth C.C. 2003. Desorption kinetics of radiocesium from subsurface sediments at Hanford Site, USA. *Geochim. Cosmochim. Acta* 67: 2893–2912

- Mihalík J., Henner P., Frelon S., Camilleri V., Fevrier L. 2012. Citrate assisted phytoextraction of uranium by sunflowers: study of fluxes in soils and plants and resulting intra-plant distribution of Fe and U. *Environ. Exp. Bot.* 77: 249-258
- Missana T., García-Gutiérrez M., Benedicto A., Ayora C., De-Pourcq K. 2014. Modeling of Cs sorption in natural mixed-clays and the effects of ion competition. *Appl. Geochem.* 49: 95-102.
- Murdock C., Kelly M., Chang L.-Y., Davison W., Zhang H. 2001. DGT as an in situ tool for measuring radiocesium in natural waters. *Environ. Sci. Technol.* 35: 4530-4535
- Murota K., Saito T., Tanaka S. 2016. Desorption kinetics of cesium from Fukushima soils. *J. Environ. Radioact.* 153: 134-140
- Nia Y., Garnier J.-M., Rigaud S., Hanna K., Ciffroy P. 2011. Mobility of Cd and Cu in formulated sediments coated with iron hydroxides and/or humic acids: a DGT and DGT-PROFS modeling approach. *Chemosphere.* 85: 1496-1504
- Nowack B., Koehler S., Schulin R. 2004. Use of Diffusive Gradients in Thin Films (DGT) in undisturbed field soils. *Environ. Sci. Technol.* 38: 1133–1138
- Okumura M., Kerisit S., Bourg I.C., Lammers L.N., Ikeda T., Sassi M., Rosso K.M., Machida M. 2018. Radiocesium interaction with clay minerals: Theory and simulation advances Post-Fukushima. *J. Environ. Radioact.* 189: 135-145
- Poinssot C., Baeyens B., Bradbury M.H. 1999. Experimental and modelling studies of caesium sorption on illite. *Geochim. Cosmochim. Acta* 63: 3217-3227
- Rigol A., Vidal M., Rauret G. 1999a. Effect of the ionic status and drying on radiocesium adsorption and desorption in organic soils. *Environ. Sci. Technol.* 33: 3788-3794
- Rigol A., Roig M., Vidal M., Rauret G. 1999b. Sequential extractions for the study of radiocesium and radiostrontium dynamics in mineral and organic soils from Western Europe and Chernobyl areas. *Environ. Sci. Technol.* 33: 887-895
- Rigol A., Vidal M., Rauret G. 2002. An overview of the effect of organic matter on soil-radiocaesium interaction: Implications in root uptake *Journal of Environmental Radioactivity* 58: 191-216
- Roig M., Vidal M., Rauret G., Rigol A. 2007. Prediction of Radionuclide Aging in Soils from the Chernobyl and Mediterranean Areas. *J. Environ. Qual.* 36: 943–952
- Siroux B., Wissocq A., Beaucaire C., Latrille C., Petcut C., Calvaire J., Tabarant M., Benedetti M.F., Reiller P.E. 2018. Adsorption of strontium and caesium onto an Na-illite and Na-illite/Na-smectite mixtures: Implementation and application of a multi-site ion-exchange model. *Appl. Geochem.* 99: 65-74

Sochaczewski Ł., Tych W., Davison B., Zhang H. 2007. 2D DGT induced fluxes in sediments and soils (2D DIFS). *Environ. Model. Software* 22: 14-23

Steinhauser G., Niisoe T., Harada K.H., Shozugawa K., Schneider S., Synal H-A., Walther C., Christl M., Nanba K., Ishikawa H., Koizumi A. 2015. Post-accident sporadic releases of airborne radionuclides from the Fukushima Daiichi nuclear power plant site. *Environ. Sci. Technol.* 49: 14028-14035

Tachi Y., Sato T., Takeda C., Ishidera T., Fujiwara K., Iijima K. 2020. Key factors controlling radiocesium sorption and fixation in river sediments around the Fukushima Daiichi Nuclear Power Plant. Part 2: Sorption and fixation behaviors and their relationship to sediment properties *Sci. Tot. Environ.* 724: 138097

Valcke E., Cremers A. 1994. Sorption-desorption dynamics of radiocaesium in organic matter soils. *Sci. Tot. Environ.* 157: 275-283

Wauters J., Sweeck L., Valcke E., Elsen A., Cremers A. 1994. Availability of radiocaesium in soils: a new methodology. *Sci. Tot. Environ.* 157: 239-248

Wissocq A., Beaucaire C., Latrille C. 2018. Application of the multi-site ion exchanger model to the sorption of Sr and Cs on natural clayey sandstone. *Appl. Geochem.* 93: 167-177

Zachara J.M., Smith S.C., Liu C., McKinley J.P., Serne R.J., Gassman P.L. 2002. Sorption of Csp to micaceous subsurface sediments from the Hanford site, USA. *Geochem. Cosmochim. Acta* 66: 193–211

Zhang H., Davison W., Knight B., McGrath S. 1998. In situ measurements of solution concentrations and fluxes of trace metals in soils using DGT. *Environ Sci Technol.* 32: 704–710